Scientific Research Publishing

Open Journal of Inorganic Chemistry, 2023, 13, 43-59
https://www.scirp.org/journal/ojic
ISSN Online: 2161-7414
ISSN Print: 2161-7406

# Hydroisomerization of *n*-Pentane over Zn-Fe-$S_2O_8^{2-}$/$ZrO_2$-$Al_2O_3$ Superacid Catalyst: Activity, Surface Analysis and the Investigation of Deactivation and Regeneration

**Huapeng Cui[1], Shengnan Li[2]**

[1]Key Laboratory of Transient Physical Mechanics and Energy Conversion Materials of Liaoning Province, Shenyang Ligong University, Shenyang, China
[2]China Petroleum Pipeline Engineering Corporation, Langfang, China
Email: cuihuapeng666@126.com

**How to cite this paper:** Cui, H.P. and Li, S.N. (2023) Hydroisomerization of *n*-Pentane over Zn-Fe- $S_2O_8^{2-}$/$ZrO_2$-$Al_2O_3$ Superacid Catalyst: Activity, Surface Analysis and the Investigation of Deactivation and Regeneration. *Open Journal of Inorganic Chemistry*, **13**, 43-59.
https://doi.org/10.4236/ojic.2023.133003

**Received:** May 5, 2023
**Accepted:** July 28, 2023
**Published:** July 31, 2023



## Abstract

The Zn and Fe modified $S_2O_8^{2-}$/$ZrO_2$-$Al_2O_3$ catalyst (Zn-Fe-SZA) was prepared and mechanisms of deactivation and methods for regeneration of as-prepared catalyst were explored with *n*-pentane isomerization as a probe reaction. The results indicated that the isopentane yield of the fresh Zn-Fe-SZA-F catalyst was about 57% at the beginning of the run, and declined gradually to 50% within 1500 min, then fell rapidly from 50% to 40% between 1500 and 2500 minutes. The deactivation of Zn-Fe-SZA catalyst may be caused by carbon formation on surface of the catalyst, sulfate group attenuation owing to reduction by hydrogen, removal of sulfur species and the loss of strong acid sites. It was found that the initial catalytic activity over Zn-Fe-SZA-T catalyst was 48%, which recovered by 84.3% as compared to that of fresh catalyst (57%). However, it showed a sharp decrease in isopentane yield from 48% to 29% within 1500 minutes, showing poor stability. This is associated to the loss of acidity caused by removal of sulfur species cannot be basically restored by thermal treatment. Resulfating the calcined catalyst could improve the acidity of catalyst significantly, especially strong acid sites, as compared with the calcined sample. The improved stability of the resulfated catalyst can be explained by: 1) eliminaton of carbon deposition to some extent by calcination process, 2) formation of improved acidic nature by re-sulfation, favoring isomerization on acidic sites, 3) restructuring of the acid and metal sites via the calcination-re-sulfation procedure.

**Keywords**

Zn-Fe, Solid Superacid, Surface Analysis, Deactivation, Regeneration, Hydroisomerization

## 1. Introduction

The trend existing and forthcoming regulations on gasoline have highlighted the need for clean and high-octane molecules in the gasoline pool. This requires a gradual replacement of aromatics in petroleum by less hazardous high-octane components. In view of the branched paraffin has higher octane numbers than linear alkanes, the use of gasoline that contains higher proportions of these compounds is an alternative to obtaining fuel with the required characteristics. Therefore, isomerization of light *n*-alkane (such as *n*-pentane) to corresponding branched paraffin is important for oil industry [1]. Both liquid and solid acid catalysts can be used for isomerization, but the commercial process changes to solid acid catalysts due to their strong acid sites, nontoxicity, non-corrosiveness, easy handling, low cost, easy to recover and recycle, and environmental considerations. Sulfated zirconia (SZ) and other sulfated metal oxides exhibit a strong acidity, appearing to be very active in catalyzing the isomerization of light *n*-alkane [2]. Unfortunately, the high initial activity of these catalysts decreases rapidly with increasing time on stream. The rapid deactivation is moderated when addition of transition metals to SZ or other sulfated metal oxides, such as Fe, Mn, Ni, Pd and Pt as promoters [3] [4]. Hsu *et al.* [5] researched the solid superacid catalyst for *n*-butane isomerization, which showed mental promoted catalysts had higher activity at lower temperatures but activation energies for butane isomerization are similar, and promotion increases the number of active sites rather than change their quality.

The superacid catalyst sulfated zirconia (SZ) has been the subject of many investigations due to its ability to activate light alkanes at lower temperatures. However, it suffers rapid deactivation when in contact with hydrocarbons. In order to improve the stability of solid sulfated zirconia, many researchers attempt to explore the reasons of its deactivation. Several factors may cause deactivation of solid SZ catalyst [6]: 1) coke formation on the surface of SZ [7], 2) reducing $Zr^{4+}$ to $Zr^{3+}$ by hydrocarbon reaction [8], 3) sulfate group attenuation owing to reduction by hydrogen and possible removal of sulfur as $H_2S$ [9], 4) reduction of the oxidation state of sulfur in the surface sulfate from $S^{6+}$ to lower oxidation states resulting in a decrease in acid strength and changes in the surface acidity [10], 5) a change in the surface phase of zirconia from tetragonal (active) to monoclinic (inactive) as a result of reaction [11], and 6) poisoning by water [12].

In our previous work [13], the Fe-Zn doped $S_2O_8^{2-}/ZrO_2$-$Al_2O_3$ (SZA) catalysts were synthesized and effects of Fe and Zn on the structure and isomerization performance of SZA were studied using *n*-pentane as a probe reaction, Fe can effectively increase *n*-alkane diffusion and reduce the activation energy of

diffusion of *n*-alkane [14]. An improved *n*-pentane isomerization performance was observed by incorporation of Fe and Zn into SZA. The isopentane yield over Zn-Fe-SZA catalyst maintains stable around 58% - 65% within 1500 min, after which the deactivation rate gets slightly faster, and the isopentane yield is decreased to 42% within 2800 min. The Fe-Zn-SZA showed a higher initial isomerization activity but its stability is still not satisfied. Therefore, in order to enhance the stability of the catalyst, it is obliged to explore the reasons for deactivation. The goal of our study is to investigate the deactivation reasons of Zn-Fe-SZA catalyst for *n*-pentane isomerization, and study the regeneration methods for renewing the activity and stability of the spent Zn-Fe-$S_2O_8^{2-}$ / $ZrO_2$-$Al_2O_3$ catalyst.

## 2. Experimental

### 2.1. Catalyst Preparation

A co-precipitated catalyst precursor was prepared from a mixed solution of $ZrOCl_2{\cdot}8H_2O$ and $Al(NO_3)_3{\cdot}9H_2O$ with a fixed ratio using $NH_4OH$ solution as a precipitating agent [15] until a final pH value of 9 - 10. The mixture thus obtained was stirred in a vessel for 1 h at room temperature. The resulted precipitates were aged for 18 h at the room temperature. The hydroxide was filtered and washed with distilled water until free of chloride and then dried at 110˚C for 12 h. Subsequently, the precursor power was impregnated with 0.75 mol·$L^{-1}$ $(NH_4)_2S_2O_8$ solution for 6 h and then filtered. The resulting solid sample was dried overnight at 110˚C (denoted at PSZA), then calcined at 650˚C for 3 h. The obtained sample with Al content of 2.5 wt% was designed as SZA.

Zn-Fe-SZA catalyst precursors were obtained by incipient wetness impregnation of the PSZA with aqueous solution of $Zn(NO_3)_2{\cdot}6H_2O$ and $Fe(NO_3)_3{\cdot}6H_2O$, simultaneously. And obtained precipitate was dried at 110˚C, then calcined at 650˚C for 3 h after extrusion into narrow strips. The obtained catalyst was designed as Zn-Fe-SZA-F.

### 2.2. Catalyst Characterization

The $N_2$ adsorption-desorption isotherms and pore diameter distribution were measured by an automatic NOVA 2000e system from Quantachrome micromeritics. X-ray diffraction (XRD) was carried out on a D/max-2200PC-X-ray diffractometer. FT-IR measurements were carried out with a Spectrum GX Fourier transform infrared spectrometer. The surface sulfur and other elements contents were analyzed by X-ray photoelectron spectroscopy (XPS) using ESCALAB MKII spectrometer. The thermal programmed desorption of $NH_3$ ($NH_3$-TPD) was used to estimate the amount and strength of acid sites formed on the surface of catalyst. The $NH_3$-TPD analysis was carried out in a CHEMBET-3000 instrument with a thermal conductivity detector. Prior to TPD measurements, samples were pretreated at −196˚C for 1 h in a flow of ultrapure $N_2$ (20 mL·$min^{-1}$) and then cooled at 100˚C. Pure $NH_3$ was introduced for about 30 min, followed by

purging with $N_2$ for 60 min at 100˚C. Subsequently, the samples were heated at a ramp of 10˚C·min$^{-1}$ up to 700˚C. $H_2$-TPR was carried out on a Builder PCA-1200 instrument with a thermal conductivity detector made by Beijing Builder Electronic Technology Co. Ltd. In addition, the sample was heated under a 20 mL·min$^{-1}$ flowing gas and the heating rate was 10˚C·min$^{-1}$. The bulk element contents of samples were determined by X-ray fluorescence (XRF) using Rigaku ZSX Primus II spectrometer. The bulk sulfur contents were analyzed by firing-correcting determination.

### 2.3. Catalytic Test

The isomerization of *n*-pentane was performed in a fixed-bed flow reactor. Prior to the reaction, the catalyst was activated. A dose of *n*-pentane was passed over the 3 g of activated catalyst under the following reaction conditions: at the temperature of 180˚C, reaction pressure of 2.0 MPa, a molar $H_2$/*n*-pentane ratio of 4:1, and a weight hourly space velocity of 1.0 h$^{-1}$. The products were analyzed by an online FL9790 gas chromatograph equipped with FID detector.

### 2.4. Catalysts Regeneration

The spent catalyst after stability test was designed Zn-Fe-SZA-D. The Zn-Fe-SZA-D catalyst was regenerated by two methods: 1) The Zn-Fe-SZA-D catalyst was calcined in static air at a temperature of 600˚C for 3 h to eliminate carbon residues on the surface and then cooled down to room temperature. The obtained sample was designed as Zn-Fe-SZA-T and the regeneration method code as calcination method. 2) The above calcined Zn-Fe-SZA-T sample was impregnated with 0.75 mol·L$^{-1}$ $(NH_4)_2S_2O_8$ solution for 6 h and then filtered and dried at 110˚C, calcined in static air at 650˚C for 3 h. The obtained sample was designed as Zn-Fe-SZA-P and the regeneration method code as sulfation method. Prior to any subsequent reaction, the catalysts were pretreated in hydrogen as mentioned in catalyst preparation

## 3. Results and Discussion

### 3.1. XRD Analysis

The XRD patterns of fresh, spent and regenerated samples were illustrated in Figure 1. All the samples showed the sharp diffraction peaks of tetragonal $ZrO_2$ at around $2\theta$ = 30.2˚, 35.6˚, 50.5˚, 60.2˚ and 74.8˚, demonstrating that the tetragonal $ZrO_2$ is predominant phase on all the samples. All the XRD patterns showed only peaks of $ZrO_2$ phases. No diffraction peak for Zn and Fe or related compounds can be observed, implying that no or very little crystalline Zn, Fe and related compounds are formed, which also indicates that Zn or Fe possibly exists in an amorphous or a better dispersion of metal oxide with small particle size [16]. For Zn-Fe-SZA-F and Zn-Fe-SZA-D, a weak peak at 63.1˚ was observed, which was assigned to $ZrO_2$ monoclinic phase, indicating that a small amount of monoclinic peak existed on the fresh and spent samples. In addition, the peak

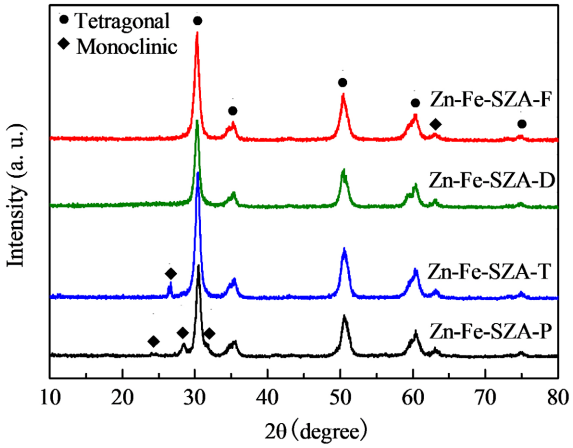


**Figure 1.** The XRD patterns of the fresh, spent and regenerated catalysts.

intensity was not changed after reaction, showing that the tetragonal $ZrO_2$ phase is stable under the isomerization conditions, which confirms the transformation of $ZrO_2$ from the metastable tetragonal phase to the monoclinic phase is not the reason for deactivation of the Zn-Fe-SZA-F. For Zn-Fe-SZA-T, low intensity peaks of the monoclinic $ZrO_2$ phase at $2\theta$ = 26.5˚ and 63.1˚ can be observed, which indicates that the transformation of $ZrO_2$ phase from tetragonal phase to monoclinic phase has happened during the regeneration of spent catalyst by calcination. While for the Zn-Fe-SZA-P, the low intensity peaks of the monoclinic $ZrO_2$ phase at $2\theta$ = 24.3˚, 28.2˚, 31.5˚ and 63.1˚, which are slightly stronger in intensity as compared with Zn-Fe-SZA-T. This may be due to the twice calcinations caused more tetragonal $ZrO_2$ transformed to monoclinic $ZrO_2$. The tetragonal phase has been reported to be the necessary phase for isomerization activity in SZ catalysts [17]. The similarity of the XRD pattern of fresh catalyst with spent catalyst, indicating that the tetragonal structure was stable under the reaction conditions. Clearly, deactivation of the Zn-Fe-SZA catalyst was not caused by a $ZrO_2$ phase change during *n*-pentane isomerization.

### 3.2. BET Analysis

The specific surface areas of fresh, spent and regenerated samples were determined from the analysis of nitrogen adsorption data performed at −196℃ according to the Bruner-Emmett-Teller method (BET method). The calculated BET values are presented in **Table 1**. It can be seen that the Zn-Fe-SZA-F catalyst showed a surface area of 89.4 $m^2 \cdot g^{-1}$. Compared with the Zn-Fe-SZA-F catalyst, the surface area of the Zn-Fe-SZA-D catalyst decreased significantly to 45.5 $m^2 \cdot g^{-1}$, accompanied by a decrease in the pore volume from 0.101 to 0.06 $cm^3 \cdot g^{-1}$ Apparently, the pores of catalyst blocked dramatically by deposition of carbon on surface of the catalyst during isomerization. The increased pore diameter for the spent sample confirms that deposited carbon blocked the smaller pores on surface of catalyst [18] [19]. In addition, the deposition of carbon would cover

**Table 1.** Texture properties of the fresh, spent and regenerated catalysts.

| Catalyst | $S_{BET}$ ($m^2 \cdot g^{-1}$) | $V_p$ ($mL \cdot g^{-1}$) | $d_p$ (nm) | $D_c^a$ (nm) |
|---|---|---|---|---|
| Zn-Fe-SZA-F | 89.3 | 0.101 | 4.5 | 8.0 |
| Zn-Fe-SZA-D | 63.7 | 0.060 | 5.3 | 6.7 |
| Zn-Fe-SZA-T | 80.6 | 0.099 | 5.1 | 7.8 |
| Zn-Fe-SZA-P | 69.8 | 0.100 | 6.7 | 6.3 |

the acid sites and mental active sites on catalysts, which is another important reason for the deactivation of catalyst.

The surface area of the Zn-Fe-SZA-T catalyst was 80.6 $m^2 \cdot g^{-1}$. As compared with the Zn-Fe-SZA-D, the surface area of the catalyst increased dramatically from 63.7 $m^2 \cdot g^{-1}$ to 90.2 $m^2 \cdot g^{-1}$, accompanied by increases in pore volume from 0.060 $mL \cdot g^{-1}$ to 0.099 $m^2 \cdot g^{-1}$, as a result of elimination of the carbon deposition. This shows that after calcining the spent catalyst, BET surface area and pore volume were basically recovered. However, the Zn-Fe-SZA-T catalyst surface was slightly lower than the fresh one, which would cause a decrease in activity as compared with that of Zn-Fe-SZA-F. The surface area of Zn-Fe-SZA-P catalyst decreased from 80.6 $m^2 \cdot g^{-1}$ to 69.8 $m^2 \cdot g^{-1}$ after resulfating Zn-Fe-SZA-T with ammonium peroxydisulfate. This is possible because the pores are blocked by sulfate species.

### 3.3. FT-IR Analysis

The infrared spectra of fresh, spent and regeneration samples are given in **Figure 2**. The broad absorption bands in the region of 3419 $cm^{-1}$ can be attributed to O-H stretching vibrations of the physically adsorbed water molecules [20]. The infrared absorption bands at 1620 $cm^{-1}$ are assigned to the deformation vibration mode of the adsorbed water [21]. The band at about 615 $cm^{-1}$ can be related to the vibration of O-Zr.

The band at 1275 $cm^{-1}$ corresponds to the antisymmetric O=S=O stretching frequency of persulfate ions bonded to $ZrO_2$. The intensity of this peak indicates the amount of $S_2O_8^{2-}$ and active acid centers formed on the catalyst surface [22] [23]. All samples exhibit the bands at 1143 and 1076 $cm^{-1}$ assigning to the symmetric O-S-O stretching mode of bidentate persulfate ions coordinated to the metal ion. The band intensity and extent of splitting reflect the proportion of active sites linked to the catalyst. The characteristic vibration peaks of S=O and S-O bonds confirm the presence of a solid superacid structure in all samples.

The fresh Zn-Fe-SZA-F catalyst had a high intensity S=O vibration band at 1275 $cm^{-1}$ and bands at 1143 and 1076 $cm^{-1}$, corresponding to S-O vibration, were sharp. The intensities and splitting of these three bands reflected the proportion of active sites in the catalyst. As compared with fresh Zn-Fe-SZA-F catalyst, the

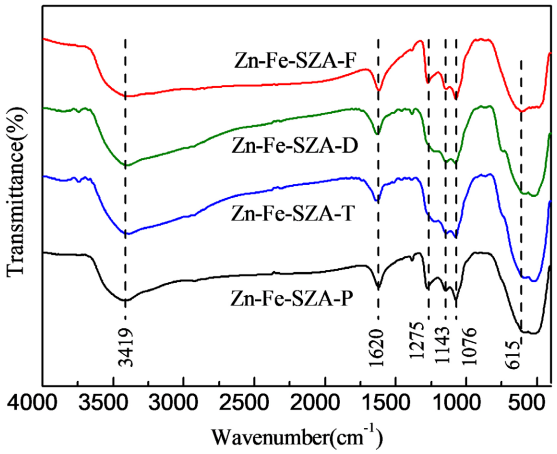


**Figure 2.** IR spectra of fresh, spent and regeneration catalysts.

S=O vibration band of Zn-Fe-SZA-D and Zn-Fe-SZA-T catalysts shifted from 1275 $cm^{-1}$ to 1239 $cm^{-1}$. In addition, the band intensity decreased significantly as compared with fresh Zn-Fe-SZA catalyst. As mentioned above, the bands observed at 1239 $cm^{-1}$ are assigned to the symmetric O=S=O stretching frequency of persulfate ions bonded to $ZrO_2$ [24], and its intensity indicates the proportion of strong acid sites linked to the catalyst. Therefore, the shift of the S=O vibration band and decrease in its intensity indicates the decrease in the acid strength and acid amount since the strong acid sites were associated with the acid sites generated by the symmetric O=S=O stretching frequency of persulfate ions bonded to $ZrO_2$. This result is consistent with the observation made by $NH_3$-TPD analysis, which will be discussed in $NH_3$-TPD analysis. The similarity of these three S=O and S-O vibration bands for the Zn-Fe-SZA-D and Zn-Fe-SZA-T demonstrates that the acid strength and acid amount could not be recovered to the level of fresh one only by calcining the spent catalyst. This result shows that the decrease in acidity was mainly due to the loss of sulfur species (See **Table 2**), indicating that subsequent resulfating of the calcined Zn-Fe-SZA-T catalyst is needed to recover the acidity of catalyst. Therefore, deactivation of catalyst mainly associated with the loss of sulfur species. As compared with Zn-Fe-SZA-T, the S=O vibration band of the Zn-Fe-SZA-P catalyst shifted from 1239 $cm^{-1}$ back to 1275 $cm^{-1}$ accompanied with significant increase in its intensity. This shows that the acid strength and acid amount could be recovered by resulfating of the calcined Zn-Fe-SZA-T catalyst.

### 3.4. XPS Analysis

In order to further clarify the deactivation reason of the Zn-Fe-SZA-F catalyst during isomerization under hydrogen atmosphere, XPS characterization was carried out to examine the changes of chemical state of sulfur species for fresh, spent and regenerated samples (**Figure 3**). The spectrum of fresh sample shows a peak at 169.8 eV, which could be assigned to $S^{6+}$ species [25]. For the Zn-Fe-SZA-D, Zn-Fe-SZA-T and Zn-Fe-SZA-P samples, the peaks for $S^{6+}$ species

**Table 2.** XPS atomic ratios of the fresh, spent and regeneration catalysts.

| Sample | | Atomic concentration (wt%) | | | | | |
|---|---|---|---|---|---|---|---|
| | | Al 2p | C 1s | Fe 2p | Zn 2p | S 2p | Zr 3d |
| Zn-Fe-SZA-F | Surface[a] | 6.37 | 5.27 | 5.37 | 2.71 | 3.76 | 55.13 |
| | Bulk[b] | 1.21 | - | 3.36 | 1.46 | 2.93[c] | 60.60 |
| Zn-Fe-SZA-D | Surface[a] | 6.11 | 7.24 | 5.26 | 2.01 | 2.92 | 52.65 |
| | Bulk[b] | 1.18 | 1.8[d] | 3.18 | 1.41 | 2.75[c] | 60.15 |
| Zn-Fe-SZA-T | Surface[a] | 6.27 | 5.67 | 4.53 | 1.82 | 2.49 | 55.84 |
| | Bulk[b] | 1.19 | - | 3.22 | 1.44 | 2.78c | 60.84 |
| Zn-Fe-SZA-P | Surface[a] | 5.07 | 5.46 | 2.10 | 1.91 | 5.07 | 54.42 |
| | Bulk[b] | 1.16 | - | 3.05 | 1.51 | 3.15[c] | 60.92 |

[a]The data obtained by XPS analysis; [b]The data obtained by XRF analysis; [c]The data obtained by firing-correcting measurement; [d]The data obtained by TG analysis.

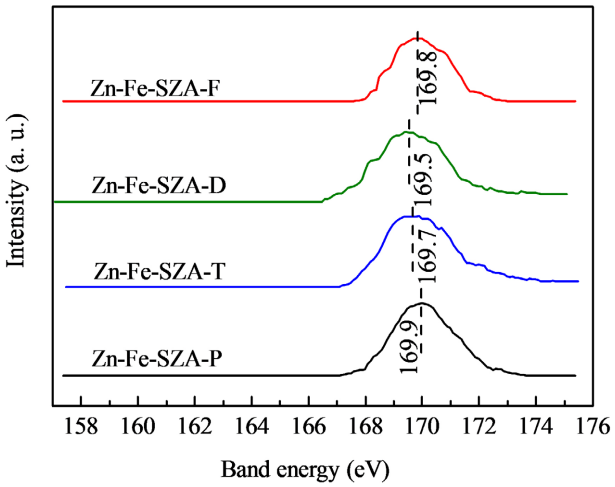


**Figure 3.** Comparison of S2p XPS profiles of fresh, spent, calcined and resulfated catalysts.

were at 169.5 eV, 169.7 eV and 169.9 eV, respectively. The difference in binding energy for $S^{6+}$ species indicates the different strength and nature of acidity [4]. The higher the binding energy for $S^{6+}$ species is, the stronger interaction between sulfates with ZA substrate and metal. Therefore, the Zn-Fe-SZA-P sample possesses the stronger acidity, which is in accordance with the FT-IR and $NH_3$-TPD analysis. No appreciable peak of S-containing species with valence different from $S^{6+}$ was observed. Samples are based on XPS measurements. For clarity, the effect of the surface elements on deactivation of catalyst will discuss together with other elemental analysis results in elemental analysis.

### 3.5. Elemental Analysis

The detailed results of bulk elemental analysis of different samples are shown in Table 2. It can be seen from Table 2 that as compared with fresh catalyst, no significant change in Fe, Al and Zr contents was observed after reaction, showing these metals were not lost during reaction and catalyst deactivation is unrelated to these elements. After reaction the surface content of Zn decreased significant from 2.71% to 2.01%. However, the bulk content of Zn almost remained unchanged. After calcining the Zn-Fe-SZA-D catalyst, the content of Zn element of catalyst was restored to the original level of the fresh catalyst. This indicates that the deposition of carbon on the surface is responsible for the decrease in surface Zn content.

A significant change in S content was observed after isomerization. The surface sulfur content of the Zn-Fe-SZA-D catalyst decreased from 3.76 to 2.92 wt%, which agrees with the trend of bulk sulfur content, which also showed a decrease from 2.93 to 2.75 wt% after isomerization. The loss of sulfur species would cause a significant decrease in the acidity of catalyst, which is in accordance with the FT-IR result. Therefore, the deactivation of catalyst is associated with the loss of sulfur species. Similar results were also found by Wolf *et al.* [17]. They had found that the sulfur content decreased from 1.65% to 1.56 wt% after reaction, and explained this phenomenon as the loss of loose-bound S species on the surface of catalysts during reaction [26]. The bulk sulfur content of the Zn-Fe-SZA-T catalyst remained unchanged as compared to the Zn-Fe-SZA-D catalyst, however, the surface sulfur content of Zn-Fe-SZA-T catalyst was decreased after calcining, which shows that re-arrangement of surface elements occurred during calcining. The Zn-Fe-SZA-P catalyst showed the highest sulfur content. It is proposed that regenerative oxidation/reduction cycles lead to a restructuring of the acid and metal sites which facilitates hydrogen migration and helps to arrest deactivation [26]. The Zn-Fe-SZA-P catalyst was obtained by sulfating the Zn-Fe-SZA-T catalyst, which had gone through calcination spent catalyst in air, impregnation with $(NH_4)_2S_2O_8$ solution, calcination in air, and reduction in $H_2$ flow. Therefore, it is reasonable to speculate that a surface re-arrangement of either the metal sites or the acid (SZ) sites on the zirconia matrix, or both, occurring during the various treatments of re-oxidatin and re-reduction processes. As a result, more persulfate ions were bonded with $ZrO_2$ in "resulfated" catalyst causing increase in sulfur content. For the Zn-Fe-SZA-P catalyst, the content of the surface elements changed much as compared with the Zn-Fe-SZA-F catalyst, which confirms a surface re-arrangement mentioned above accured after regenerative oxidation/reduction cycles.

A sharp increase in surface carbon content (about 1.97 wt% obtained by XPS analysis and 1.8 wt% obtained by TG analysis) was observed for the Zn-Fe-SZA-D catalyst due to deposition of carbon. Clearly, the deposition of carbon would cause blockage of some pores of catalyst and decrease the surface area (Table 1), cause coverage of active acid and metal sites. As a result, activity of the catalyst

for isomerization would be declined. Therefore, carbon deposition is another important reason for the deactivation of catalyst. After calcining the Zn-Fe-SZA-D catalyst, the surface carbon content of catalyst decreased to that of original fresh catalyst showing the carbon deposition could be eliminated nearly completely by calcination.

### 3.6. TG Analysis

For measuring the content of the coke deposited on the catalyst during the reaction, TG analysis of fresh and spent catalysts were performed. As can be seen from **Figure 4**, for the Zn-Fe-SZA-F catalyst, two distinct weight losses were observed at temperature below 250˚C and above 650˚C. The weight loss occurred below 250˚C can be attributed to the loss of weakly adsorbed water from the hydroxide into zirconium oxide. From 250˚C to 650˚C, the weight loss continued but at a very low rate. However, the second distinct weight loss region, which began at 650˚C, is associated to the decomposition of sulfate species [27] [28]. Sameer Vijay [17] also reported that this loss is due to evolution of $SO_2$ owing to decomposition of the sulfate species.

In comparison with the Zn-Fe-SZA-F catalyst, TG curve for the Zn-Fe-SZA-D catalyst exhibits an additional distinct weight loss region in the temperature range of 250˚C - 500˚C, which can be attributed to the oxidation of the carbon deposits arising from the reaction ($C + O_2 \rightarrow CO_2$, $\Delta H_{298} = -393.5$ kJ/mol) [29]. The weight loss of this region is about 1.8 wt%, demonstrating that the carbon deposition on the Zn-Fe-SZA-D catalyst is about 1.8 wt%. This value agrees with the result (about 1.97 wt%) obtained by XPS analysis. Based on the TG analysis, it can be concluded that the regeneration temperature should lower than the decomposition temperature of sulfate species (650˚C) and higher than the combustion temperature which could totally eliminate carbon deposition on surface of the catalyst (500˚C). Therefore, for eliminating the coke deposited on the Zn-Fe-SZA-D, the appropriate calcination temperature is between 500˚C and 650˚C.

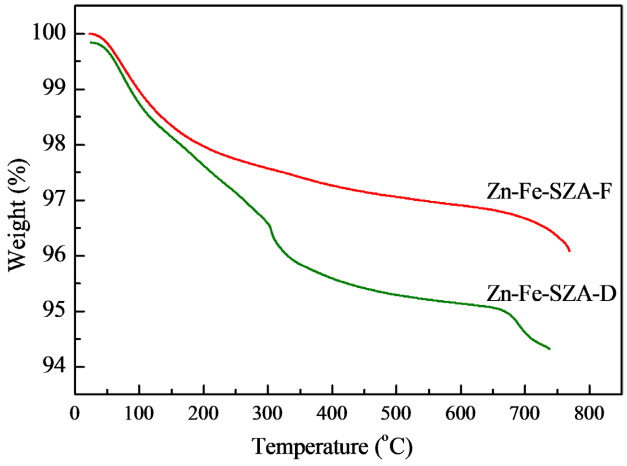


**Figure 4.** TG curves of fresh and spent catalysts calcinated in air.

### 3.7. $NH_3$-TPD Analysis

The $NH_3$-TPD curves of fresh, spent and regeneration samples are shown in Figure 5. It can be seen from Figure 5 that the $NH_3$-TPD curves of samples were deconvoluted into individual desorption peaks of Gaussian shape. The resulting peaks were classified and grouped into two types of acid sites with different acidic strength, weak and strong, according to the temperature of the peak maximum. The temperature range for the peak maxima of the weak acid sites was set between 150˚C and 400˚C, and for the strong acid sites above 400˚C. Probably, the weak acid sites derived from weak Lewis acid sites and terminal the symmetric O-S-O stretching mode of bidentate persulfate ions coordinated to the metal ion, and the strong acid sites were associated with the acid sites generated by the symmetric O=S=O stretching frequency of persulfate ions bonded to $ZrO_2$. The strong acid sites provide the active centers of the isomerization reaction [30]. The Zn-Fe-SZA-F catalyst showed an obvious strong acid peak at 480˚C. However, the position of strong acid site peak shifted to lower temperature (460˚C) and the area below the curves of the Zn-Fe-SZA-D and Zn-Fe-SZA-T catalysts decreased as compared to the Zn-Fe-SZA-F catalyst, indicating the acid strength and amount decreased after reaction and could not be recovered by elimination of deposits. This is in accordance with result obtained by the FT-IR analysis. The possible reason for this is due to the loss of sulfur species during the reaction (Table 2), which would lead to a poor isomerization performance. For the Zn-Fe-SZA-P catalyst, the position of strong acid site peak shifted to higher temperature of 520˚C as compared to the Zn-Fe-SZA-F catalyst. In addition, the area below the curve of the Zn-Fe-SZA-P catalyst is recovered to the level of the fresh Zn-Fe-SZA-F catalyst. The above discussion indicating the strength of strong acid and amount of acid could be recovered by resulfating of the calcined Zn-Fe-SZA-T catalyst.

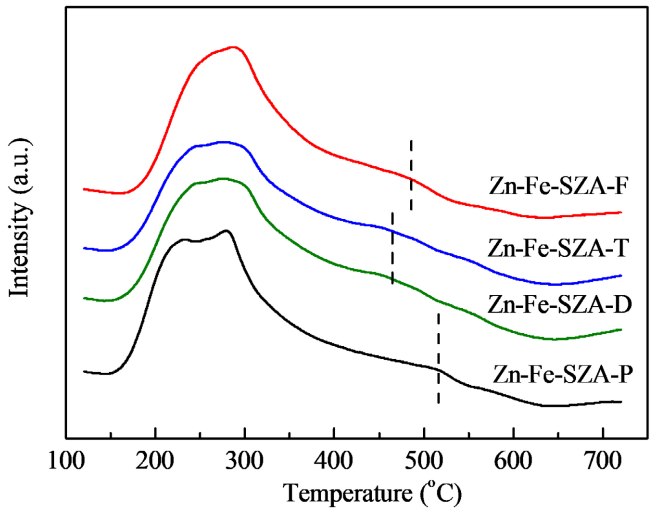


Figure 5. $NH_3$-TPD curves of the fresh, spent and regeneration catalysts.

### 3.8. Catalyst Activity

Figure 6 shows the activity of the fresh, spent and regenerated samples at a reaction temperature of 180˚C, a pressure of 2.0 MPa, a hydrogen/hydrocarbon molar ratio of 4:1, and a MHSV of 1.0 $h^{-1}$. For the Zn-Fe-SZA-F catalyst, the isopentane yield was about 57% at the beginning of the run, and declined gradually to about 50% within 1500 min, which showed a decline of 9.1%. However, between 1500 and 2500 minutes, isopentane yield fell rapidly from 50% to 40%, which showed a decline of 20.0%. The fresh catalyst showed a high initial activity, but poor stability. These observations are similar to those reported previously [31].

The Zn-Fe-SZA-T catalyst showed a sustained decline in activity during *n*-pentane isomerization. Within 1500 minutes, the isopentane yield over the Zn-Fe-SZA-T catalyst decreased sharply from 48% to 29%, which showed a decline of 39.6%. As compared to fresh catalyst (57%), the recovery rate of initial catalytic activity reached 84.3% demonstrating the elimination of carbon by calcining spent catalyst is necessary for catalytic activity regeneration. As compared to the spent catalyst (40%), the catalytic activity increased by 22.5% upon elimination of deposit carbon. This confirms that carbon deposition is one important reason for deactivation of catalyst. In general, large polynuclear aromatics in feed mixtures tend to be coke formers. Olefinic compounds promote coke formation, possibly either by direct interaction or by acting as hydrogen acceptors. Although, light hydrocarbons are of low molecular weight, they can polymerize and dehydrocyclize to form higher-boiling aromatics and coke [6]. In addition, carbon deposition is confirmed by XPS and TG analysis, which would cover part of the active acid and metal sites on the surface of the catalyst. This would lead to deactivation of some metal and acid sites (Table 2) and cause decrease in

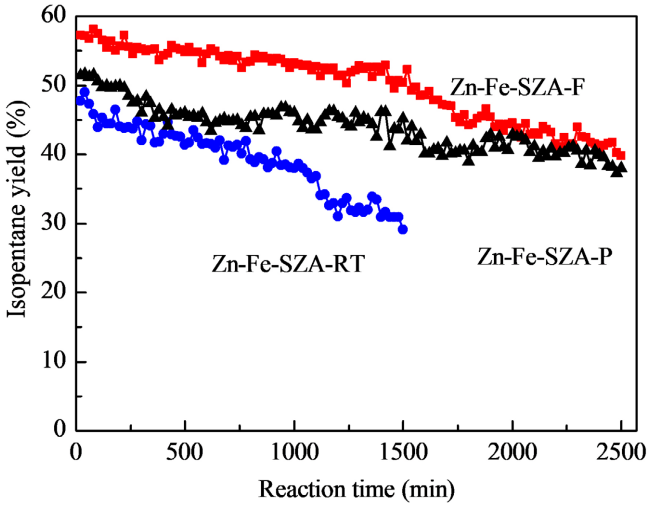


Figure 6. Stability test of fresh, calcined" and "resulfated" Zn-Fe-SZA catalysts for *n*-pentane isomerization. (Reaction conditions: $T$ = 180˚C, $p$ = 2.0 MPa, $H_2$/*n*-pentane = 4, WHSV = 1.0 $h^{-1}$.)

surface area (Table 1). Therefore, carbon deposition is one important reason for deactivation. However, the Zn-Fe-SZA-T catalyst showed a lower activity with a poor stability. This demonstrates that the catalytic activity could not be basically recovered by elimination carbon deposition of the Zn-Fe-SZA-D. The surface sulfur content of the Zn-Fe-SZA-D catalyst decreased from 3.76 wt% to 2.92 wt%, This agrees with the trend of bulk sulfur content, which is also showed a decrease from 2.93 wt% to 2.75 wt% after isomerization. The loss of sulfur species caused a significant decrease in acid amount (FT-IR), especially strong acid sites (XPS and $NH_3$-TPD analysis), therefore, deactivation of catalyst might associate with the loss of sulfur species and strong acid. As is well known, calcination can eliminate carbon deposition, but the removed sulfate species cannot be restored by thermal treatment [32]. This was confirmed by FT-IR, XPS and $NH_3$-TPD analysis, which showed that the strength and acid amount of the Zn-Fe-SZA-F catalyst decreased after reaction, which is possibly associated with the poor stability and declined initial activity for the Zn-Fe-SZA-T. As is well known, the strong acid sites provide the active centers of the isomerization reaction [30]. Therefore, the loss of acid strength and acid amount due to removal of sulfur species during the reaction is another main reason for deactivation. And the deactivation is irreversible. The above discussion indicating that in order to restore the activity of catalyst, the acid strength and acid amount should be recovered.

For the resulfated Zn-Fe-SZA-P catalyst, the isopentane yield was 52% at the beginning of the run, which is lower than that of fresh catalyst. As compared to fresh catalyst (57%), the recovery rate of initial catalytic activity reached 91.2% demonstrating the catalytic activity was basically recovered. As compared to the calcined catalyst (48%), the initial catalytic activity increased by 8.3% upon re-sulfation the calcined catalyst. However, the isopentane yield is declined gradually to 38% from 52% within 2500 min; the decline is much slower than that of fresh one. As compared to fresh Zn-Fe-SZA-F catalyst, the resulfated Zn-Fe-SZA-P catalyst showed a better stability, but the initial activity was a little lower. This can be interpreted by the traditional bifunctional reaction mechanism for isomerization of pentane, which involves hydrogenation-dehydrogenation on metal sites, isomerization and/or cracking on acidic sites, and diffusion of the olefinic intermediates between acidic and metal sites. The metal sites dehydrogenate the alkanes into alkenes, which are protonated on the Brønsted acid sites yielding carbenium ions. After rearrangement, these carbenium ions desorb from the acid sites as alkenes and are hydrogenated on the metal sites yielding saturated reaction products. With catalysts lacking acid or metal sites, the corresponding process becomes the rate-determining step [31]. Therefore, the synergistic interaction between metal sites and acidic sites plays an important role in isomerization. The low catalytic activity for the Zn-Fe-SZA-P catalyst, may be explained by its higher surface sulfur content (Table 2), which would cover some of the metal sites and therefore weaken the hydrogenation-dehydrogenation performance of catalyst.

The improved stability for the Zn-Fe-SZA-P catalyst is due to an enhanced acid strength, which favors isomerization. Vijay and Wolf [17] have studied pentane isomerization over Pt-promoted SZ catalysts and reported that upon repeated regenerations, an increase in stability was observed. They explained that regenerative oxidation/reduction cycles lead to a restructuring of the acidic and metal sites, which facilitates hydrogen migration and helps to arrest deactivation. The surface metals and sulfur contents obtained by the XPS analysis changed significantly as compared to the Zn-Fe-SZA-F catalyst, which confirmed the restructuring of the acidic and metal sites. In summary, the catalyst obtained by sulfation method showed better stability, although the initial activity was slightly lower as compared with fresh one, which demonstrated the important role of acid amount and acid strength. The improved stability of the resulfated catalyst can be explained by: 1) eliminaton of carbon deposition to some extent by calcination process; 2) formation of improved acidic nature by re-sulfation, favoring isomerization on acidic sites; 3) restructuring of the acid and metal sites via the calcination-re-sulfation procedure.

## 4. Conclusion

The mechanisms of deactivation and methods for regeneration of the as-prepared Zn-Fe-SZA-F catalyst were explored with *n*-pentane isomerization as a probe reaction. For the Zn-Fe-SZA-F catalyst, the isopentane yield was about 57% at the beginning of the run, and declined gradually to about 50% and 40% within 1500 and 2500 min, respectively. All the XRD patterns showed only peaks of $ZrO_2$ phases and small amount of monoclinic peak existed on the fresh and spent samples. The crystalline tetragonal structure of $ZrO_2$ remained unchanged, which is not the reason for deactivation. The Zn-Fe-SZA-T catalyst calcined in air at 600˚C for 3 h and then reduced in $H_2$ at 300˚C for 3 h under 1 $h^{-1}$ (GHSV) showed initial catalytic activity of 48%. As compared to fresh catalyst (57%), the recovery rate of initial catalytic activity reached 84.3% demonstrating that carbon elimination by calcining spent catalyst is necessary for catalytic activity regeneration. The carbon deposition is confirmed by XPS and TG analysis, which would also cover part of the active acid and metal sites on the surface of the catalyst. The loss of sulfur species caused poor stability and declined initial activity for the Zn-Fe-SZA-T catalyst as compared to the fresh one. Resulfating the calcined catalyst could improve the acidity of catalyst significantly, especially strong acid sites (XPS and $NH_3$-TPD analysis). However, the resulfated catalyst showed better stability, although the initial activity was slightly lower as compared with the fresh one, which demonstrated the important role of acid amount and acid strength. The improved stability of the resulfated catalyst can be explained by: 1) eliminaton of carbon deposition to some extent by calcination process; 2) formation of improved acidic nature by re-sulfation, favoring isomerization on acidic sites; 3) restructuring of the acid and metal sites via the calcination-re-sulfation procedure.

## Conflicts of Interest

The authors declare that they have no known competing financial interests or personal relationships that could have appeared to influence the work reported in this paper.

## References


[1] Chen, X.P., Du, Y.Q., Chen, C.L., Xu, N.P. and Mou, C.Y. (2006) Highly Active and Stable *n*-Pentane Isomerization Catalysts without Noble Metal Containing: Al- or Ga-Promoted Tungstated Zirconia. *Catalysis Letter*, **111**, 187-193. https://doi.org/10.1007/s10562-006-0146-3

[2] Urzhuntsev, G.A., Ovchinnikova, E.V., Chumachenko, V.A., Yashnik, S.A., Zaikovsky, V.I. and Echevsky, G.V. (2014) Isomerization of *n*-Butane over Pd-$SO_4$/$ZrO_2$ Catalyst: Prospects for Commercial Application. *Chemical Engineering Journal*, **238**, 148-156. https://doi.org/10.1016/j.cej.2013.08.092

[3] Song, H., Meng, Y., Song, H.L. and Li, F. (2016) Acid Strength of Ni-$S_2O_8^{2-}$/$ZrO_2$ Catalyst and Its Catalytic Activity for *n*-Pentane Isomerization. *Russian Journal Applied Chemistry*, **89**, 670-678. https://doi.org/10.1134/S1070427216040224

[4] Zhang, L., Gao, Y.F., Bai, X.R., He, L.W., Fu, W.Q. and Tang, T.D. (2023) Ni Catalyst on ZSM-22 Nanofibers Bundles with Good Catalytic Performance in the Hydroisomerization of n-Dodecane. *Fuel*, **357**, Article ID: 129885. https://doi.org/10.1016/j.fuel.2023.129885

[5] Hsu, C.Y., Heimbuch, C.R., Armes, C.T. and Gates, B.C. (1992) The Effect of Sulfate Contents on the Surface Properties of Iron-Manganese Doped Sulfated Zirconia Catalysts. *Journal of Chemical Society*, *Chemical Communications*, **22**, 1645-1646. https://doi.org/10.1039/c39920001645

[6] Yang, Y.C. and Weng, H.S. (2009) The Role of $H_2$ in *n*-Butane Isomerization over Al-Promoted Sulfated Zirconia Catalyst. *Journal of Molecular Catalysis A*: *Chemical*, **304**, 65-70. https://doi.org/10.1016/j.molcata.2009.01.025

[7] Song, H., Zhao, L.L., Wang, N. and Li, F. (2016) Isomerization of *n*-Pentane over La-Ni-$S_2O_8^{2-}$/$ZrO_2$-$Al_2O_3$ Solid Superacid Catalysts: Deactivation and Regeneration. *Applied Catalysis A*: *General*, **526**, 37-44. https://doi.org/10.1016/j.apcata.2016.08.003

[8] Klose, B.S., Jentoft, F.C., Joshi, P., Annette, T., Robert, S., Subbotina, I.R. and Kazansky, V.B. (2006) *In Situ* Spectroscopic Investigation of Activation, Start-Up and Deactivation of Promoted Sulfated Zirconia Catalysts. *Catalysis Today*, **116**, 121-131. https://doi.org/10.1016/j.cattod.2006.01.036

[9] Moreno, J.A. and Poncelet, G. (2001) *n*-Butane Isomerization over Transition Metal-Promoted Sulfated Zirconia Catalysts: Effect of Metal and Sulfate Content. *Applied Catalysis A*: *General*, **210**, 151-164. https://doi.org/10.1016/S0926-860X(00)00802-4

[10] Wang, H.G., Shi, G.L., Yu, F. and Li, R.F. (2016) Mild Synthesis of Biofuel over a Microcrystalline $S_2O_8^{2-}$/$ZrO_2$ Catalyst. *Fuel Processing Technology*, **14**, 9-13. https://doi.org/10.1016/j.fuproc.2016.01.021

[11] Zhao, Z.H. and Ran, J.F. (2015) Sulphated Mesoporous $La_2O_3$-$ZrO_2$ Composite Oxide as an Efficient and Reusable Solid Acid Catalyst for Alkenylation of Aromatics with Phenylacetylene. *Applied Catalysis A*: *General*, **503**, 77-83. https://doi.org/10.1016/j.apcata.2015.01.023

[12] Zhang, R. and Liu, Y.F. (2000) The Influence of Water on $SO_4^{2-}/ZrO_2$ Typed Solid Superacid Catalyzed Pentane Isomerization. *Chemical Engineering of Oil and Gas*, **29**, 53-55.

[13] Song, H., Cui, H.P., Song, H.L. and Li, F. (2016) The Effect of Zn-Fe Modified $S_2O_8^{2-}/ZrO_2$-$Al_2O_3$ Catalyst for *n*-Pentane Hydroisomerization. *Research on Chemical Intermediates*, **42**, 3029-3038. https://doi.org/10.1007/s11164-015-2195-y

[14] Xiang, J.N., Zhang, W., Zhang, H.P., Wang, S.Z., Ma, M.X., Wang, Y.T., Wang, Y., Dai, W.J., Fan, B.B., Zheng, J.J., Ma, J.H. and Li, R.F. (2023) Effect of Fe Substitution over ZSM-48 on Performance of *n*-Dodecane Hydroisomerization and Distribution of Isomers. *Solid State Sciences*, **142**, Article ID: 107250. https://doi.org/10.1016/j.solidstatesciences.2023.107250

[15] Reddy, B.M., Sreekanth, P.M., Yamada, Y. and Kobayashi, T. (2005) Modified Zirconia Solid Acid Catalysts for Organic Synthesis and Transformations. *Journal of Molecular Catalysis A*: *Chemical*, **227**, 81-89. https://doi.org/10.1016/j.molcata.2004.10.011

[16] El-Shall, M.S., Abdelsayed, V., Khder, A., Hassan, H., El-Kaderi, H.M. and Reich, T.E. (2009) Metallic and Bimetallic Nanocatalysts Incorporated into Highly Porouscoordination Polymer MIL-101. *Journal of Material Chemistry*, **19**, 7625-7631. https://doi.org/10.1039/b912012b

[17] Vijay, S. and Wolf, E.E. (2004) A Highly Active and Stable Platinum-Modified Sulfated Zirconia Catalyst: 1. Preparation and Activity for *n*-Pentane Isomerization. *Applied Catalysis A*: *General*, **264**, 117-124. https://doi.org/10.1016/j.apcata.2003.12.036

[18] Sah, B. and Sengupt, S. (2015) Influence of Different Hydrocarbon Components in Fuel on the Oxidative Desulfurisation of Thiophene: Deactivation of Catalyst. *Fuel*, **15**, 679-686. https://doi.org/10.1016/j.fuel.2015.02.078

[19] Kong, X.J., Wang, G.Y., Du, X.B., Lu, L., Li, L. and Chen, L.G. (2012) Coking Deactivation and Regeneration of $Cs_2O$-$P_2O_5/SiO_2$ for Aziridine Synthesis. *Catalysis Communication*, **27**, 26-29. https://doi.org/10.1016/j.catcom.2012.06.020

[20] Guo, Q. and Wang, T. (2014) Preparation and Characterization of Sodium Sulfate/Silica Composite as a Shape-Stabilized Phase Change Material by Sol-Gel Method. *Chinese Journal of Chemical Engineering*, **22**, 360-364. https://doi.org/10.1016/S1004-9541(14)60047-1

[21] Azambre, B., Zenboury, L., Weber, J.V. and Burg, P. (2010) Surface Characterization of Acidic Ceria-Zirconia Prepared by Direct Sulfation. *Applied Surface Science*, **256**, 4570-4581. https://doi.org/10.1016/j.apsusc.2010.02.049

[22] Ahmed, M.A. (2011) Surface Characterization and Catalytic Activity of Sulfated-Hafnia Promoted Zirconia Catalysts for n-Butane Isomerization. *Fuel Process Technology*, **92**, 1121-1128. https://doi.org/10.1016/j.fuproc.2011.01.008

[23] Li, J.Q. (2004) Study on Preparation of $S_2O_8^{2-}/ZrO_2$-$Ce_2O_3$ Solid Superacid and Catalytic Synthesis of Butyl Acetate. *Journal of University of South China*, **18**, 48-51.

[24] Sohn, J.R., Lee, S.H. and Lim, J.S. (2006) New Solid Superacid Catalyst Prepared by Doping $ZrO_2$ with Ce and Modifying with Sulfate and Its Catalytic Activity for Acid Catalysis. *Catalysis Today*, **116**, 143-150. https://doi.org/10.1016/j.cattod.2006.01.023

[25] Bianchi, C.L., Ardizzone, S. and Cappelletti, G. (2004) Surface State of Sulfated Zirconia: The Role of the Sol-Gel Reaction Parameters. *Surface and Interface Analysis*, **36**, 745-748. https://doi.org/10.1002/sia.1753

[26] Yan, Y.C. and Weng, H.S. (2010) Al-Promoted Pt/ $SO_4^{2-}$ /$ZrO_2$ with Low Sulfate Content for n-Heptane Isomerization. *Applied Catalysis A*: *General*, **384**, 94-100. https://doi.org/10.1016/j.apcata.2010.06.010

[27] Bautista, P., Faraldos, M., Yates, M. and Bahamonde, A. (2007) Influence of Sulphate Doping on Pd/Zirconia Based Catalysts for the Selective Catalytic Reduction of Nitrogen Oxides with Methane. *Applied Catalysis B*: *Environmental*, **71**, 254-261. https://doi.org/10.1016/j.apcatb.2006.08.020

[28] Yu, G.X., Zhou, X.L., Liu, F., Li, C.L., Chen, L.F. and Wang, J.A. (2009) Effect of Isopropanol Aging of $Zr(OH)_4$ on n-Hexane Isomerization over Pt- $SO_4^{2-}$ /$Al_2O_3$-$ZrO_2$. *Catalysis Today*, **148**, 70-74. https://doi.org/10.1016/j.cattod.2009.02.045

[29] Wang, Y.L., Luo, G.H., Xu, X. and Xi, J.J. (2014) Deactivation of Supported Skeletal Ni Catalyst and Effect of Regeneration Temperature on Its Catalytic Performance. *Catalysis Communication*, **57**, 83-88. https://doi.org/10.1016/j.catcom.2014.07.034

[30] Zhang, W., Zhang, H.P., Ma, M.X., Wang, S.Z., Xiang, J.N., Wang, Y., Dai, W.J., Fan, B.B., Zheng, J.J. and Li, R.F. (2023) Synthesis of Ga-Modified ZSM-48 with Improved Hydroisomerization Performance *n*-Dodecane. *Reaction Chemistry & Engineering*, **8**, 2481-2490. https://doi.org/10.1039/D3RE00278K

[31] Guo, K., Ma, A.Z., Wang, Z.J., Li, J.Z., Wu, B.F., Liu, T. and Li, D.D. (2022) Investigation of *n*-Heptane Hydroisomerization over Alkali-Acid-Treated Hierarchical Pt/ZSM-22 Zeolites. *New Journal of Chemistry*, **46**, 16752-16763. https://doi.org/10.1039/D2NJ02820D

[32] Martins, A., Silva, J.M. and Ribeiro, M.F. (2013) Influence of Rare Earth Elements on the Acid and Metal Sites of Pt/HBEA Catalyst for Short Chain *n*-Alkane Hydroisomerization. *Applied Catalysis A*: *General*, **466**, 293-299. https://doi.org/10.1016/j.apcata.2013.06.043